Paleohydrological changes during the last deglaciation in Northern Brazil

Jérémy Jacob, Yongsong Huang, Jean-Robert Disnar, Abdelfettah Sifeddine, Mohammed Boussafir, Ana Luiza Spadano Albuquerque, Bruno Turcq

Paleohydrological changes during the last deglaciation in Northern Brazil

Jérémy Jacob[1,2*], Yongsong Huang[1], Jean-Robert Disnar[2], Abdelfettah Sifeddine[3], Mohammed Boussafir[2], Ana Luiza Spadano Albuquerque[4] and Bruno Turcq[3,4].

[1] Department of Geological Sciences, Brown University, Providence, Rhode Island 02912, USA.

[2] Institut des Sciences de la Terre d'Orléans - UMR 6113 du CNRS, Bâtiment Géosciences, 45067 Orléans Cedex 2, France.

[3] IRD/Bondy, 32 avenue Henry Varagnat, 93143 Bondy Cedex, France.

[4] Departamento de Geoquimica, Universidade Federal Fluminense, Morro do Valonguinho s/n, 24020-007 Niteroi, RJ, Brazil.

[*] Corresponding author. E-mail address: *jeremy.jacob@univ-orleans.fr*

Abstract

We here report a reconstruction of hydrological balance variations in Northern Brazil for the last 20 ka deduced from the δD values of aquatic and land plant molecules extracted from the sediment infill of Lake Caçó. Our reconstructed precipitation, lake water isotope ratio and evaporation-evapotranspiration isotope effect allow us to obtain an estimate of moisture balance, and, to a lesser extent, precipitation amount and seasonality changes. During the end of the Last Glacial Maximum (LGM, between ca. 20 and 17.3 ka), high δD values and smaller fractionation of leaf waxes indicate an arid to semi-arid climate with a long lasting dry season. An abrupt change towards much wetter conditions occurred within ca. 500 years from 17.3 to 16.8 ka, as shown by a 50 ‰ decrease in D/H ratios and a marked increase in H isotopic fractionation of leaf waxes. This abrupt isotopic change coincides with a major transformation from savanna-dominated vegetation to humid rain forest around the lake, based on pollen data. Comparisons with other paleo-precipitation records from South American sites indicate that late glacial humid conditions were controlled by intensification of the ITCZ and/or a southward shift of its mean position across our study site. Our isotope data show only a small rise in aridity during Younger Dryas event (13 to 11.5 ka). Although the Holocene was not screened in details, D/H ratios of terrestrial and aquatic compounds show near constant offsets, suggesting stable and relatively humid climate conditions during this period.

Keywords: hydrological balance, relative humidity, seasonality, South America, hydrogen isotope ratios, lake sediments, Lake Caçó, D/H.

1. Introduction

The tropics are key areas for past and present climate dynamics because this region is the main heat engine and water vapour source of the Earth. Recent studies indicate that past variations in the water vapour cycle over tropical South America are closely related to oceanic and atmospheric circulation patterns at global scale (Peterson et al., 2000; Wang et al., 2004; Cruz et al., 2005). Nonetheless, there is not yet a clear consensus on the role of the tropics in driving global climate variability and on the possible extratropical feedbacks (Stoecker et al., 2003). An important atmospheric system that controls the tropical climate variations is the InterTropical Convergence Zone (ITCZ). Previous studies have indicated that the mean positioning of the ITCZ has shifted significantly on seasonal, decadal and longer timescales (Martin et al., 1997; Ronchail et al., 2002; Wang et al., 2004). In order to track past ITCZ shifts and changes in intensity, we have explored the sedimentary infill of Lake Caçó. This lake is located in Northern Brazil, on the eastern edge of Amazon rain forest, where the ITCZ shifts from its winter to summer position (Fig. 1). It is therefore highly sensitive to mean positioning of the ITCZ.

There are major controversies remaining on the occurrence of wet/dry episodes in South America and their impacts on continental ecosystems, biological diversity and biogeochemical cycling (CH_4, CO_2 and H_2O). For example, a globally drier climate is suspected for the LGM. The extent to which this supposedly dry episode impacted the Amazon rainforest surface is strongly debated (Colinvaux et al., 2000; Turcq et al., 2002). Similar to the LGM, the tropical extension and influence of the Younger Dryas (YD) cold reversal, as defined in the Northern Hemisphere, is not fully elucidated in the South American tropics.

Most of these controversies arise from the lack of pertinent parameters allowing the quantitative estimate of humidity changes. For instance, broadly defined pollen classes

include several taxa that can colonize various habitats. Furthermore, pollen data are interpreted as changes in vegetation distribution that are affected by atmospheric pCO_2, temperature, humidity and soil properties, thus avoiding any quantitative reconstruction. Similarly, marine sedimentary cores record regional conditions inland and buffer spatial discrepancies.

In order to address the question of humidity variations in Southern America since the last deglaciation, we apply for the first time in the South American tropics the combination of hydrogen isotopic composition (δD)[a] of aquatic and land plant molecules preserved lake sediments. As it has recently been shown, the δD values of sedimentary palmitic ($n-C_{16}$) and behenic ($n-C_{22}$) acids as well as short chain *n*-alkanes capture the δD of meteoric waters (Huang et al., 2002, 2004; Sachse et al., 2004; Hou et al., 2006), that is related to precipitation amount in the tropics (Dansgaard, 1964). The δD of leaf wax lipids produced by land plants, such as triacontanic acid ($n-C_{30}$) and other long chain fatty acids (Eglinton and Hamilton, 1967), although dependent on the δD of meteoric waters (Sachse et al., 2006), is also affected by evaporation and transpiration processes (Sauer et al., 2001; Liu and Huang, 2005). As a matter of fact, the δD of leaf wax lipids has been recently used to track humidity changes in tropical Africa from marine sediments (Schefuß et al., 2005). In a first approximation, the fractionation factor between the δD values of lipids from land plants and the calculated δD values of water allows us to estimate evapotranspiration. Here, we present the first hydrogen isotopic record from Lake Caçó sediments in North-eastern Brazil covering the last 20,000 cal. yr, which brings new insights into the interconnecting mechanisms between ocean-atmosphere-continent in the tropics.

[a] $\delta D = [D/H_{sample} / D/H_{standard} - 1] \times 1000$. VSMOW is the standard for δD, expressed as permil (‰).

2. Settings

The study site (Lake Caçó, Maranhaõ State, Brazil) is located about 80 km from the Atlantic coast and close to the Equator (Fig. 1, 2°58'S, 43°25'W and 120 m above sea-level). The local present-day climate is tropical humid with pronounced seasonality. Average rainfall annually reaches 1500 mm and mostly occurs during the rainy season, from November to May (see Ledru et al., 2006). Rainfall distribution and river discharge in this region are impacted by the seasonal migration of the InterTropical Convergence Zone (ITCZ; Figure 1; Hastenrath, 1990). Modern δD of precipitation in Sao Luiz (the closest IAEA/WMO[b] station), range from -10 ‰ (during austral summer) to 0 ‰ (during austral winter). The mean annual temperature is 26 °C. The lake (surface: ca. 2.5 km²; volume: 8.6 10^6 m^3) occupies a former river valley within a dune field and collects waters from a watershed of ca. 15 km². The maximum water depth recorded is 12 m during the wet season and ca. 11 m during the dry season. The lake is river charged during the rainy season and both river and groundwater charged during the dry season. The outflow rate being on average 0.4 $m^3.s^{-1}$, the calculated turnover time of waters is ca. 0.65 year. Modern vegetation that is governed by dune dynamics and topography ranges from littoral steppe vegetation "*restinga*" to sandy savanna "*cerrado"* with "*restinga*" species admixed (Ledru et al., 2001). Most of the primary production from terrestrial and aquatic plants occurs during the rainy season.

[b] IAEA/WMO : International Atomic Energy Agency/World Meteorological Organization (2004). Global Network of Isotopes in Precipitation. The GNIP Database. Accessible at: http://isohis.iaea.org

3. Sample collection and lipid analyses

Core MA-98-3 (6m long) was collected in 1998 in the middle of the lake (10 m depth) with a vibracorer (Martin et al., 1995) and kept under 5°C until analysis. We have observed some compaction in the first meter of sediment but the water-sediment interface has been preserved. 31 two centimetre thick samples were selected for this study. The samples were oven-dried at 50°C for 12 hours before crushing.

The method for lipid preparation is the same as described in Huang et al. (2002) and Hou et al. (2006). Two grams of powdered sediment were used for free lipids extraction using an accelerated solvent extractor (ASE200, Dionex) with CH_2Cl_2:CH_3OH (1:1). The carboxylic acids were separated from the total extract using solid phase extraction on Aminopropyl Bond Elute© cartridges according to Huang et al. (1999). Then, they were converted into fatty acid methyl esters using anhydrous 2 % HCl in CH_3OH. Hydroxyl acids were removed using silica gel column chromatography with CH_2Cl_2 in order to further purify the fatty acid methyl esters and avoid chromatographic coelution.

The δD and $\delta^{13}C$ measurements of individual fatty acid methyl esters were performed by GC-C-IRMS according to Huang et al. (2002) and Hou et al. (2006). A Hewlett Packard 6890 GC interfaced to a Finnigan Delta+ XL stable isotope spectrometer through high-temperature pyrolysis and combustion reactors were used for hydrogen and carbon isotopic analysis. Ultra high purity hydrogen and carbon dioxide gas with known δD and $\delta^{13}C$ values were pulsed three times at the beginning and end of each analysis. The H_3 factor was determined daily.

The accuracy of hydrogen isotope measurements was evaluated using a mixture of four *n*-alkane standards (nC_{16}, nC_{18}, nC_{20}, and nC_{30}) with offline measured δD values (acquired from Arndt Schimmelmann, Indiana University). This mixture was analysed every 6 injections and the standard deviation for these isotopic standards was on average less than ±

4.5 ‰ during the course of this study. Because these results were satisfactory, we did not proceed to a normalization of δD results.

The reported δD and $\delta^{13}C$ values for fatty acids methyl esters were corrected by mathematically removing the isotopic contribution of carbon and hydrogen atoms added during methylation. The δD (-123 ‰) and $\delta^{13}C$ (-35.62 ‰) values of the added methyl group were determined by acidifying and then methylating the disodium salt of succinic acid with a predetermined δD and $\delta^{13}C$ values (using TC/EA-IRMS). Triplicate (for deuterium) and duplicate (for ^{13}C) analyses of the samples resulted in an overall precision better than ± 3 ‰ (δD) and ± 0.35 ‰ ($\delta^{13}C$) for nC_{16}, nC_{22} and nC_{30} fatty acid methyl esters.

4. Results

4.1. Age model

The age model (Figure 2) is constrained by six radiocarbon ages (Table 1) that have been performed on bulk organic matter by acceleration mass spectrometry (AMS) at the Beta Analytic Laboratory (Florida, USA). Due to the poor soil cover presently found in the region, and the globally dry climate experienced in the region during the last 20 ka, we consider that few or even no aged organic carbon contributed to the sediment. In addition, the substratum is exclusively made of inorganic sand dunes (quartz and kaolinite) and, locally, laterites, in the region. This excludes a contribution from fossil organic matter. Interpolated ages were calculated using the intercept of the mean conventional age interval with the calibration curve of ^{14}C (CALIB version 4.3, Stuiver and Reimer, 1993; Stuiver et al., 1998). In combination with radiocarbon dates obtained on other cores drilled in the lake centre (Sifeddine et al., 2003; Ledru et al., 2005) we assume the sedimentation continuous over the record with mean sedimentation rates from 0.15 to 0.24 cm/yr in the lower half of the core and from 0.01 to 0.05 cm/yr in the upper half of the core.

4.2. Downcore variations

The δD variations for palmitic (δD_{PA}), behenic (δD_{BA}) and triacontanic (δD_{TA}) fatty acids as well as their $\delta^{13}C$ values are plotted against time in Figure 3. For convenience, the δD values (‰ VSMOW) and $\delta^{13}C$ values (‰ VPDB) are given as ‰ (per mil) in the text.

The $\delta^{13}C$ values for nC_{16} fatty acid start at ca. -24 ‰ in the oldest samples and then decrease down to -32 ‰ around 12 ka before increasing up to -29 ‰ at 8 ka and then remaining stable. The general trend depicted by behenic acid $\delta^{13}C$ values is comparable to that of palmitic acid. However, a mean isotopic enrichment of ca. 6 ‰ for behenic acid as compared to palmitic acid is recorded in samples younger than 17 ka. $\delta^{13}C$ values for triacontanic acid average -31 ‰ in the 20-19 ka interval, reaches up to -29 ‰ between 19 and 17 ka and then remains around -32 ‰ until present.

δD_{PA} values range from -240 to -160 ‰. The 20-19 ka interval shows strong variations in δD_{PA} between -240 and -190 ‰. Then, δD_{PA} values remain around ca. -190 ‰ between 19 and 17 ka and around -180 ‰ from 17 to 13.5 ka. δD_{PA} values become lower between 13.5 and 11.8 ka (-190/-200 ‰) before slightly increasing up to -180 ‰ at ca. 11.5 ka. For more recent samples, the values progressively decrease from -180 ‰ down to -200 ‰. δD_{BA} shows a comparable trend as δD_{PA} with a mean enrichment of ca. 40 ‰. The detailed differences between the two records will be discussed in paragraph 5.3. The δD_{TA} values are higher during the 20-17 ka time interval as compared to younger samples (average -128 ‰ compared to -157 ‰, respectively), the highest values being recorded around 17 ka. A slight increase in δD_{TA} values up to -150 ‰ occurs around 12-13 ka and offsets the YD. This increase is followed by a minima of δD_{TA} (-170 ‰) at 11 ka. From 10 ka to the present, both δD_{TA} and δD_{PA} slightly increase up to ca. -160 and -190 ‰, respectively.

5. Discussion

5.1. Origin of palmitic, behenic, and triacontanic acids

Previous results acquired from bulk and molecular geochemistry attest to a large contribution of higher plant organic matter to the sediment (Jacob, 2003; Jacob et al., 2004; 2005). However, the use of molecular markers allows for distinguishing between different source organisms within a complex organic matter.

Triacontanic acid, as other long chain *n*-alkyl lipids, originates from leaf epicuticular waxes (Eglinton and Hamilton, 1967). High $\delta^{13}C$ values (ca. – 30 ‰) recorded from 20 to 17 ka for this compound attests to a great contribution of C4 plants and/or lower stomatal conductance of C3 plants due to dryer conditions (Farquhar et al., 1989). After 17 ka, the vegetation mainly consists of C3 plants as attested by rather low $\delta^{13}C$ values for triacontanic acid.

Behenic acid, as well as other mid-length chain *n*-alkyl lipids, is mainly derived from aquatic macrophytes (Ficken et al., 2000). In the case of Lake Caçó, emergent aquatic macrophytes are abundant and mainly consist of *Eleocharis sp.* (spike-rush), a Cyperaceae that develops around the lake between 1 and 3 m depth (Jacob, 2003).

Palmitic acid is produced by most organisms. Nevertheless, it has been shown that this compound is rapidly degraded in leaves or litters when produced by higher plants (Marseille et al., 1999; Bourdon et al., 2000; Disnar et al., 2005). Therefore, higher plant-derived palmitic acid is unlikely to reach the sediment. A dominantly aquatic origin for palmitic acid in lake sediments is further supported by the fact that δD values of this compound found in lake surface sediments track lake water δD values in 33 lakes in the Eastern North America (Huang et al., 2002). Furthermore, the evolution of δD and $\delta^{13}C$ values for palmitic and behenic acids show comparable trends, distinct from those of triacontanic acid, hence

indicating a common reservoir different from those of higher plants both for hydrogen and carbon.

The difference in carbon isotopic discrimination recorded between the end of the LGM and more recent samples by both palmitic (ca. -25/-30 ‰) and behenic acids (ca. -24/-36 ‰) is coherent with a similar shift displayed by the $\delta^{13}C$ of phytoplanktonic lipids in an African tropical lake (Sacred Lake, Kenya; Huang et al., 1999). Increased $\delta^{13}C$ values for palmitic and behenic acids at the end of the LGM are attributed to lower atmospheric pCO_2 and higher pH leading to inorganic carbon limitation (low dissolved CO_2) in the lake waters. Lower lake level and smaller volume may have also induced nutrient concentration and higher productivity, causing further draw down of dissolved and CO_2 and higher $\delta^{13}C$ values of algal biomass. During the late glacial and after, higher $[CO_2]_{aq}$ due to higher dissolved CO_2 favoured the isotopic discrimination by aquatic organisms, leading to lower $\delta^{13}C$ values. This isotopic effect was enhanced by a stronger carbon input from C3 plants to the lake that entailed a lowering of the $\delta^{13}C$ values of DIC in the lake waters, via remineralization of organic carbon.

5.2. Uncertainties in linking δD of lipids with environmental parameters

The complex way allowing an isotopic signal depending on a given set of climatic parameters to be preserved in sedimentary lipids is summarized in Figure 4. Although non-exhaustive, this diagram allows understanding the different factors that influence the final isotopic signal in sedimentary archives, and therefore, the sources of uncertainty. These can be divided into environmental, biological and geological factors.

5.2.1. Environmental factors

Environmental factors controlling the hydrogen isotopic composition of water used by organisms for lipid biosynthesis are the same as those affecting the $\delta^{18}O$ composition of water used for carbonate precipitation. These factors have been reviewed recently in Leng and Marshall (2004). The δD of rainfall for a given region is dependent on the δD of the source water (the ocean), isotopic effects due to temperature and latitude, continentality and altitude but also the amount of rainfall and the seasonality of precipitation. Since Lake Caçó is located in the tropics, close to the Atlantic Ocean and at a low altitude, the δD of precipitation is mostly dependent on the amount and seasonality of rainfall. Then, meteoric waters suffer runoff, infiltration and recharge of aquifers. The isotopic composition of soil water is affected by evaporation and transpiration processes that are influenced by wind speed, insolation and vegetation cover. If the δD of lake waters is considered, the limnology of the lake must be taken into account (von Grafenstein, 2002: Leng and Marshall, 2004). Wherever the lake waters are in steady state (i.e. reflect the isotopic composition of rainfall) depends on the ratio between the watershed and the lake surfaces, the turnover time of water in the lake and evaporation processes.

5.2.2. Biological factors

The soil or lake water is then used by organisms for their biosynthesis. The isotopic fractionation between plant water and environmental water depends on physiological factors affecting water uptake, transport and evapotranspiration, considering aerial plants for this latter (Sessions et al., 2006; Smith and Freeman, 2006). The main isotopic fractionation occurs during lipid biosynthesis, depending on biosynthetic pathways (*n*-alkyl lipids versus isoprenoids for example) and compartmentalization of water use. This leads to net a

biological fractionation of more than 150 ‰ between environmental waters and lipids (Sessions et al., 2006 and references therein).

5.2.3. Geological factors

Organic matter produced from different sources within the watershed is then transported towards the lake and suffers differential degradation. It is mixed with autochthonous organic matter within the water column before entering the sediment. Considering these phenomenon, it is worthwhile accounting for the residence time of organic matter within each compartment, inducing a delayed record of the sedimentary archive to climatic variations. In conclusion, the sediment integrates organic-derived paleoclimatic information in both time and space.

Despite these numerous pitfalls, one can assume that original isotopic signals are preserved within sedimentary organic matter, i.e. that the correlation between the δD values of sedimentary lipids and the δD values of past environmental waters is dependent on few variables that can be constrained by using lipids of distinct origins. The challenge remains to deconvolute these different effects and to reconstitute past climate variability. It is what we tried in the following discussion.

5.3. Paleoenvironmental interpretation of compound-specific isotopic trends

Interpretation of our isotopic records from Lake Caçó is based on a number of established relationships and/or assumptions:

(i) Consistent with surface sediment calibration from eastern North American lakes, δD values of palmitic (δD_{PA}) and behenic (δD_{BA}) acids record the lake water isotope ratios (Huang et al., 2002, 2004; Hou et al., 2006). The constant D/H fractionation factor is 0.829 ± 0.014 between palmitic acid and lake waters (Huang et al., 2002) and 0.8681 between behenic acid and lake waters (Hou et al., 2006). For this later an error of ± 0.0414 is assumed. This value corresponds to the maximum discrepancy for the behenic acid/lake water fractionation factor between the slope and the intercept of the calibration curve described by Hou et al. (2006). The hydrogen isotopic composition of the lake waters is calculated from δD_{PA} as follows:

$$\delta D_{watPA} = (\delta D_{PA} + 170) / 0.829$$

and from δD_{BA} as follows :

$$\delta D_{watBA} = (\delta D_{BA} + 136.4) / 0.8681$$

The reconstructed hydrogen isotopic evolutions of the lake waters are reported in Figure 3. Considering for each value the analytical error ($\Delta\delta D_{PA}$ and $\Delta\delta D_{BA}$) and the error affecting the isotopic fractionation factor (0.014 for palmitic acid and 0.0414 for behenic acid), the resulting errors are calculated as follow:

$$\Delta\delta D_{watPA} = (\Delta\delta D_{PA} \times 0.829 + 0.014 \times \delta D_{PA}) / 0.829^2$$

and

$$\Delta\delta D_{watBA} = (\Delta\delta D_{BA} \times 0.8681 + 0.0414 \times \delta D_{BA}) / 0.8681^2$$

δD_{watPA} values between 20 ka and 17 ka are highly variable within a -85 / -20 ‰ range. Then, and up to ca. 13.5 ka, δD_{watPA} values are relatively constant above -20 ‰. After

the 13.5-11.8 interval characterized by values lower than -20 ‰, δD_{watPA} values raise at ca. -15 ‰ in a single sample before decreasing down to -45 ‰ and then increasing towards -20 ‰. The variations of δD_{watBA} values are less marked except in the 20-17 ka interval.

Although δD_{watPA} and δD_{watBA} records are in general agreement, again indicating that palmitic and behenic acids both record the isotopic composition of the lake waters, the best fit between the two curves occurs for samples belonging to the 17–13 ka interval, that corresponds to the most humid conditions recorded in the region for the last 20 ka (see paragraph 5.3.2.). Higher values of δD_{watBA} relative to δD_{watPA} recorded in the other intervals are not well understood although they could result from an enrichment in deuterium due to evapotranspiration affecting emerged plants (the supposed producers of behenic acid), when lake level lowers. Therefore, we use the δD_{wat} derived from δD_{PA} (δD_{watPA}) as an estimate of the δD values of the lake waters. In the tropics, the main parameter that controls the δD of meteoric waters is the amount of precipitation ("amount effect"; Dansgaard, 1964). This parameter is therefore used as an estimate of precipitation, with high δD_{watPA} values indicating reduced precipitation and reversely.

(ii) We assume that lake water (≈ mean annual precipitation) represents the water used by land plants, since there is currently no alternative to reconstruct groundwater used by land plants. The variations in $\alpha_{TA/wat}$, the fractionation factor between δD_{TA} and δD_{watPA} ($\alpha_{TA/wat} = [\delta D_{TA}+1000]/[\delta D_{watPA}+1000]$), result from the enrichment of leaf waters in deuterium as compared to meteoric waters. Higher $\alpha_{TA/wat}$ values result from higher soil evaporation and leaf transpiration (Huang et al., 2004; Sachse et al., 2004, 2006; Hou et al., 2006). Error bars displayed on the $\alpha_{TA/wat}$ curve in Figure 3 are calculated by combining the analytical error on δD_{TA} and the calculated error on δD_{watPA} as follow:

$$\Delta\alpha_{TA/wat} = (\Delta\delta D_{watPA} \times (\delta D_{TA} + 1000) + (\delta D_{watPA} + 1000) \times \Delta\delta D_{TA})/ (\delta D_{watPA} + 1000)^2$$

$\alpha_{TA/wat}$ values are high (between 0.9 and 0.94) during the 20-17 ka period. After a sudden decrease down to 0.86, $\alpha_{TA/wat}$ values remain stable around 0.85 up to 13.5 ka. The 13.5-11.8 ka interval is characterized by slightly higher coefficient (ca. 0.867) that remain around this figure in more recent samples, except for single points.

(iii) The δD_{TA} parameter is affected both by δD_{wat} and by soil evaporation and leaf transpiration that cause a deuterium enrichment of plant leaf water: hence the value is higher under low relative humidity conditions and reversely (Yapp and Epstein, 1982). In order to decipher relative changes in relative humidity, we converted differences in δD_{TA} into differences in relative humidity, using the equation of Yapp and Epstein (1982): $\delta D_{TAa} - \delta D_{TAb} = 124 (h_a - h_b)$. δD_{TAa} and δD_{TAb} are the δD_{TA} values during periods a and b and h_a and h_b are the relative humidity that prevailed during times a and b. If this relationship, which was established for a single species at a given time, can be directly applied to a whole ecosystem (without taking account differences in evapo-transpiration due to forest/savanna successions for example) and remains valid over longer periods, it allows us obtaining an order of magnitude for humidity changes. Since this approach raises a large number of uncertainties, we did not report any uncertainty estimate.

5.4. Evolution of climatic conditions in the region

5.4.1. The end of Last Glacial Maximum

High δD_{TA} values (mean = -129 ‰) during the 20-19 ka interval (Figure 5a) result from a reduced hydrological balance (i.e. less precipitation and more evaporation leading to dry conditions). Using the equation of Yapp and Epstein (1982), the relative humidity is reduced by ca. 30 % at this time, when referring to the late glacial interval (e.g., 15 ka), taken as a reference (100 %). The rather high $\delta^{13}C$ for palmitic acid at this time most probably result from carbon limitation in the lake waters due to dry/arid conditions in the surrounding area. The highly variable δD_{watPA} (~ from -84.87 to -19.49 ‰; Fig. 5b) and $\alpha_{TA/wat}$ values (~ from 0.89 to 0.94) during this interval indicate that these conditions result from a combination of high evaporation and severe rainfalls (Figure 5b-5c). In fact, we interpret the low δD_{watPA} values during the 20-19 ka phase as resulting from episodic rainfalls. Sporadic but strong showers during a short rainy season allowed the existence of ephemeral lakes within sand dunes (Jacob et al., 2004). Within these ephemeral lakes, opportunistic phytoplanktonic communities developed during the short rainy season and captured an isotopic signal attesting to high precipitation. This short rainy season was followed by a long dry season with strong evaporation rates, as indicated by the high figures of $\alpha_{TA/wat}$.

The 19-17.3 ka period is characterized by lower precipitation than previously (δD_{watPA} increases up to ~ -34 ‰) accompanied by still high evapotranspiration (mean $\alpha_{TA/wat}$ ~ 0.91). This suggests slightly drier conditions than before with a maximum around 17.3 ka (δD_{TA} ~ 104 ‰). The calculated average relative humidity over this time period is reduced by 40 % with respect to the late glacial period. We interpret these results as a decrease of the rainy season length and still high evapotranspiration rates.

Our results are in agreement with previous work on cores collected in the same lake (Figure 5d-e). The very low AP/NAP ratios (arboreal against herbaceous pollens) during the considered time span indicate sparse vegetation dominated by grasses, typical of semi-arid climate (Ledru et al., 2001; 2002). This is also depicted by low $\delta^{13}C$ values for triacontanic acid that attest to a strong contribution of C4 plants and/or lower stomatal conductance of C3 plants (Figure 3). Increased quartz fluxes into the sediment at these times result from the intensification of eolian dune transport, a phenomenon that only occurs when the dry season lasts more than four months (Sifeddine et al., 2003). The presence of sandy sub-horizontal to oblique parallel laminations confirms the occurrences of flash floods during events of heavy rainfalls.

5.4.2. The abrupt climate change at late glacial

Between 17.3 and 16.8 ka, a rapid transition from arid/semi-arid conditions to humid conditions is reflected in the large decrease in δD_{TA} values. Then, during the late glacial period (from 16.8 to 13.5 ka), the enhanced precipitation (δD_{watPA} ~ -15 ‰) and lower soil evaporation and leaf transpiration ($\alpha_{TA/wat}$ ~ 0.85) enables the establishment of humid conditions (δD_{TA} ~ -160 ‰). During this period, pollen results show an increase of forest percentages dominated by Myrtaceae (Figure 5d and 5e), providing evidence for the development of a humid forest, in agreement with lower figures of triacontanic acid $\delta^{13}C$ values that reflect a stronger contribution of C3 plants.

5.4.3. The Younger Dryas and the Holocene

Climatic conditions appear slightly drier during the 13.5-11.8 ka time period, with δD_{TA} values reaching -158 ‰ indicating relative moisture reduced by 7 % as compared to the late glacial. The δD_{watPA} values exhibit a shift toward -21 ‰ coupled to a shift of the $\alpha_{TA/wat}$

values (maximum 0.87). These figures are interpreted as sporadic showers during a shorter rain season coupled with enhanced evaporation, as during the 20-19 ka interval, but to a lesser extent. In the meantime lower AP/NAP ratios indicate the replacement of the humid forest by open vegetation. It is worthwhile noting that triacontanic acid $\delta^{13}C$ does not exhibit a stronger contribution of C4 plants at this time, as opposed to the end of LGM. A sedimentary hiatus in a marginal core is noted and corresponds to the lowering of the lake level (Sifeddine et al., 2003). This episode is also characterized by higher quartz fluxes, probably of eolian origin, that point to a longer dry season (Sifeddine et al., 2003). During the period dated between 11.8 to 10 ka (Preboreal), δD_{TA}, δD_{watPA} and $\alpha_{TA/wat}$ values reach similar figures as during the late glacial, indicating similar hydrological conditions and accompanied by a discrete increase in arboreal pollen percentages. Then, the δD_{TA} values slightly increase through the early Holocene up to -161 ‰, illustrating a drying trend.

5.5. Regional integration within South American records

The changes in humidity evidenced in the sedimentological sequence of Lake Caçó provide the first continuous continental record in northern South America for the last 20 ka. It allows improved chronostratigraphic correlation of other paleoenvironmental time-series (e.g., vegetation changes) with our well-dated record of reconstructed paleohumidity.

Our results suggest that drier conditions prevailed at the end of the LGM in the region and attest to a probable reduction of the eastern border of the rainforest. They are consistent with the pattern of vegetation distribution proposed for the LGM (Adams and Faure, 1998). The drier mean climate probably originates from a weakening of the ITCZ and of the global hydrological cycle during the LGM. Moreover, the stronger seasonality would indicate a northward shift of the ITCZ due to a stronger pole-equator temperature gradient in the North hemisphere. The heavy rainfalls at the end of LGM would be related to interannual climate

variability during episodes when ITCZ, which was on average at a northernmost position, occasionally reached its present-day southern position.

The late glacial humid period, which is marked by an abrupt increase of precipitation and humidity at ca. 17 ka around Lake Caçó, is also recorded in the north-eastern region by travertine and speleothem active phases (Auler and Smart 2001, Wang et al., 2004; Figure 5g). It is also synchronous with the increase in the Fe/Ca ratio in a sediment core from the north-eastern Brazilian continental margin, which corresponds to increased terrigenous inputs related to more humid conditions in the hinterland (Figure 5f; Arz et al., 1998; 1999). This paleoclimate change is interpreted as a warmer sea-surface temperature episode that began with Heinrich event 1 (Arz et al., 1998). This global climatic event provoked changes in Atlantic Ocean circulation resulting in the intensification of the ITCZ and an increased moisture transport to the north-eastern South America hinterlands.

The reinforcement of these humid conditions from 15 to 13.5 ka (e.g. the Bølling-Allerød period), marked by the stability of moisture, corresponds to the beginning of lacustrine sedimentation in Lake Carajas (Sifeddine et al., 2001) and in several Brazilian records (Sifeddine et al., 1998, Auler and Smart, 2001). It is explained by a southward shift of the ITCZ which could be related to a cold reversal in the Northern hemisphere while Antarctic temperature remained stable (Fig. 5i, j).

The YD is marked by a weak decrease of precipitation and relative humidity that can be attributed to more intense evapotranspiration. Drier conditions are also reported in the Bolivian cordillera (van't Veer et al., 2000) A reduction of 60 % of the Amazon discharge, as compared to the modern flow, is noticed from the Amazon fan sediments (Figure 5h, Maslin and Burns, 2000) and reduced precipitations in northern Amazonia (Peterson et al., 2000) accompanied by the development of a dry savanna are inferred from the Cariaco Trench (Haug et al., 2001; Hughen et al., 2004). Oppositely, the YD has been interpreted as more

humid from marine cores from northern Brazil (Figure 5f, Arz et al., 1999; Behling et al., 2000). These results indicate a southern position of ITCZ which probably reached higher Southern Hemisphere latitudes during the summer of this hemisphere than its present-day shift. Based on δD data, we interpret this period as resulting from a shorter humid season, which agrees with a southern position of ITCZ in Southern Hemisphere summer.

The Preboreal period is characterized by reduced precipitation and even more reduced evaporation leading to more humid conditions in Lake Caçó region. This episode coincides with active phases of speleothems and travertines growth in the State of Bahia (Figure 5g, Wang et al., 2004) that attest to a rapid return of humid conditions in the north-eastern tip of Brazil.

6. Conclusion

Our results provide an estimate of the humidity variations in a South American tropical lake since the last deglaciation. By combining hydrogen isotope measurements on aquatic and terrestrial lipids, we show the potential of this approach to deconvolute the effects of precipitation (amount and seasonality) and evapotranspiration on the humidity. In addition, this approach would allow in certain cases the estimation of changes in seasonality of precipitation, a parameter that remains hard to discriminate in paleorecords. Despite the numerous approximations involved in our study (integration in time and space of hydrological processes, few controls on intimate physical, chemical and biological mechanisms), the outstanding correlation of our hydrogen isotope records with independent data shows the potential of this approach to track past hydrological changes in the tropics. Our ability to track more sensible hydrological changes will depend on future work on calibration that are now required in the tropics.

The comparison with other proxy records for the same period underlines the role of ITCZ position in climate changes. ITCZ position is controlled by interhemispheric gradients of temperature, insolation and ocean dynamics. Our data suggest that abrupt changes in regional climate in the tropics can be due to shifts in the ITCZ position. The sharp increase in humidity at ca. 17 ka is thought to coincide with Heinrich event 1. High humidity levels are maintained up to ca. 13.5 ka and may be related to a cooling of the Northern Hemisphere while Antarctic temperature remained quite stable. Such conditions should push ITCZ southward. The still high Southern Hemisphere summer insolation at that time also contributed directly to this humid climate phase.

Acknowledgements

This research was sponsored by a Travel Scholarship attributed by the European Association of Organic Geochemists (EAOG) to J.J. The study of Lake Caçó sediments results from a programme PALEOTROPICA supported by an IRD (France)-CNPq (Brazil) convention and an ISTO (UMR 6113 du CNRS, France)-UR055 (PALEOTROPIQUE-IRD) cooperation. The research at Brown University is supported by funds from the Earth System History Program at the National Science Foundation to Y.H. (NSF0081478, 0318050, 0318123, 0402383). The authors wish to thank A. Schimmelmann, A. Sessions, F. Palhol and A. Mangini for their constructive comments on a previous version of the manuscript.

REFERENCES CITED

Adams, J.M., Faure, H., 1998. A new estimate of changing carbon storage on land since the Last Glacial Maximum based on global land ecosystem reconstruction. Global Planet. Change 16-17, 3-24.

Arz, H.W., Pätzold, J., Wefer, G., 1998. Correlated millennial-scale changes in surface hydrography and terrigenous sediment yield inferred from Last-Glacial marine deposits off Northeastern Brazil. Quat. Res. 50, 157-166.

Arz, H W., Pätzold, J., Wefer, G., 1999. Climatic changes during the last deglaciation recorded in sediment cores from the northeastern Brazilian Continental Margin. Geo-Marine Lett. 19, 209-218.

Auler, A. S., Smart, P. L., 2001. Late Quaternary paleoclimate in semiarid northeastern Brazil fromU-series dating of travertine and water-table Speleothems. Quat. Res. 55, 159–167.

Behling, H., Arz, H. W., Pätzold, J., Wefer, G., 2000. Late Quaternary vegetational and climate dynamics in northeastern Brazil, inferences from marine core GeoB 3104-1. Quat. Sci. Rev. 19, 981-994.

Bourdon S., Laggoun-Défarge F., Maman O., Disnar J.-R., Guillet B. Derenne S., Largeau C., 2000. Organic matter sources and early diagenetic degradation in a tropical peaty marsh (Tritrivakely, Madagascar). Implications for environmental reconstruction during the Sub-Atlantic. Org. Geochem. 31, 421-438.

Colinvaux, P.A., De Oliveira, P.E., Bush, M.B., 2000. Amazonian and neotropical plant communities on glacial time-scales: The failure of the aridity and refuge hypotheses. Quat. Sci. Rev. 19, 141-169.

Cruz Jr, F.W., Burns, S.J., Karmann, I., Sharp, W.D., Vuille, M., Cardoso, A.O., Ferrari, J.A., Silva Dias, P.L., Viana Jr, O., 2005. Insolation-driven changes in atmospheric circulation over the past 116,000 years in subtropical Brazil. Nature 434, 63-66.

Dansgaard, W., 1964. Stable isotopes in precipitation. Tellus 16, 436-468.

Disnar, J. R., Stefanova, M., Bourdon S., Laggoun-Défarge, F., 2005. Sequential fatty acid analysis of a peat core covering the last two millennia (Tritrivakely lake, Madagascar): diagenesis appraisal and consequences for palaeoenvironmental reconstruction. Org. Geochem. 36, 1391-1404.

Eglinton, G., Hamilton, R.J., 1967. Leaf epicuticular waxes. Science 156, 1322–1335.

Farquhar G. D., Ehleringer J. R., Hubick K. T., 1989. Carbon isotope discrimination and photosynthesis. Annu. Rev. Plant Physiol. Plant Mol. Biol. 40, 503–537.

Ficken, K.J., Li, B., Swain, D.L., Eglinton, G., 2000. An *n*-alkane proxy for the sedimentary input of submerged/floating freshwater aquatic macrophytes. Org. Geochem. 31, 745-749.

Grafenstein, U. von., 2002. Oxygen-isotope studies of Ostracods form deep lakes. The Ostracoda: Applications in Quaternary Research. Geophysical Research Monograph 131, 249-266.

Hastenrath, S., 1990. Decadal-scale changes of the circulation in the tropical Atlantic sector associated with Sahel drought. Int. J. Climatol. 10, 459-472.

Haug, G.H., Hughen, K.A., Sigman, D.M., Peterson, L.C., Röhl, U., 2001. Southward migration of the Intertropical Convergence Zone through the Holocene. Science 293, 1304-1308.

Hou, J., Huang, Y., Wang, Y., Shuman, B., Oswald, W. W., Faison, E., Foster, D. R. 2006, Postglacial climate reconstruction based on compound-specific D/H ratios of fatty acids from Blood Pond, New England, Geochem. Geophys. Geosyst., 7, Q03008, doi:10.1029/2005GC001076.

Huang, Y., Street-Perrott, F.A., Perrott, F.A., Metzger, P., Eglinton, G., 1999. Glacial-interglacial environmental changes inferred from the molecular and compound-specific $\delta^{13}C$ analyses of sediments from Sacred Lake, Mt. Kenya. Geochim. Cosmochim. Ac. 63, 1383–1404.

Huang, Y., Shuman, B., Wang, Y., Webb III, T., 2002. Hydrogen isotope ratios of palmitic acid in lacustrine sediments record late Quaternary climate variations. Geology 30, 1103–1106.

Huang, Y., Shuman, B., Wang, Y., Webb III, T., 2004. Hydrogen isotope ratios of individual lipids in lake sediments as novel tracers of climatic and environmental change: a surface sediment test. J. Paleolimnol. 31, 363-375.

Hughen, K.A., Eglinton, T.I., Xu,L., Makou, M., 2004. Abrupt Tropical Vegetation Response to Rapid Climate Changes. Science 304, 1955-1959.

Jacob, J., 2003. Enregistrement des variations paléoenvironnementales depuis 20000 ans dans le Nord Est du Brésil (Lac Caço) par les triterpènes et autres marqueurs organiques. PhD thesis, Université d'Orléans, 296p. http://tel.ccsd.cnrs.fr/documents/archives0/00/00/29/42/index_fr.html

Jacob, J., Disnar, J.R., Boussafir, M., Sifeddine, A., Albuquerque, A.L.S., Turcq, B., 2004. Major environmental changes recorded by lacustrine sedimentary organic matter since the Last Glacial Maximum under the tropics (Lagoa do Caçó, NE Brazil). Palaeogeogr., Palaeoclim., Palaeoeco. 205, 183-197.

Jacob, J., Disnar, J.R., Boussafir, M., Sifeddine, A., Albuquerque, A.L.S., Turcq, B., 2005. Pentacyclic triterpene methyl ethers in recent lacustrine sediments (Lagoa do Caçó, Brazil). Org. Geochem. 36, 449-461.

Ledru, M.P., Cordeiro, R.C., Dominguez, J.M.L, Martin, L., Mourguiart, P., Sifeddine, A., Turcq, B., 2001. Late-glacial cooling in Amazonia as inferred from pollen at Lagoa do Caçó, Northern Brazil. Quat. Res. 55, 47-56.

Ledru, M.P., Mourguiart, P., Ceccantini, G., Turcq, B., Sifeddine, A., 2002. Tropical climates in the game of two hemispheres revealed by abrupt climatic change. Geology 30, 275-278.

Ledru, M.P., Ceccantini, G., Gouveia, S.E.M., López-Sáez, J.A., Pessenda, L.C.R., Ribeiro, A.S., 2006. Millenial-scale climatic and vegetation changes in a northern Cerrado (Northeast, Brazil) since the Last Glacial Maximum. Quat. Sci. Rev. 25, 1110, 1126.

Leng, M.J, Marshall, J.D., 2004. Palaeoclimate interpretation of stable isotope data from lake sediment archives. Quat. Sci. Rev. 23, 811, 831.

Liu, W., Huang, Y., 2005. Compound specific D/H ratios and molecular distributions of higher plant leaf waxes as novel paleoenvironmental indicators in the Chinese Loess Plateau. Org. Geochem. 36, 851-860.

Martin, L., Flexor, J.M., Suguio, K., 1995. Vibrotestemunhador leve. Construçao, utilizaçao e potencialidades. Rev. IG. Sao Paulo, 16, 59-66.

Martin, L., Mourguiart, P., Sifeddine, A., Soubiès, F., Wirrmann, D., Suguio, K., Turcq, B., 1997. Astronomical forcing of contrasting rainfall changes in tropical South America between 12,400 and 8800 cal yr BP. Quat. Res. 47, 117-122.

Marseille F., Disnar J. R, Guillet B., Noack, Y., 1999. *n*-Alkanes and free fatty acids in humus and A1 horizons of soils under beech, spruce and grass in the Massif Central (Mont-Lozère) France. Eur. J. Soil Sci., 50, 433-441.

Maslin, M.A., Burns, S.J., 2000. Reconstruction of the Amazon basin effective moisture availability over the past 14,000 Years. Science 290, 228-2287.

North Greenland Ice Core Project members, 2004. High-resolution record of Northern Hemisphere climate extending into the last interglacial period. Nature 431, 147-151.

Peterson, L.C., Haug, G.H., Hughen, K.A., Röhl, U., 2000. Rapid changes in the hydrologic cycle of the Tropical Atlantic during the Last Glacial. Science 290, 1947-1951.

Petit, J.R., Jouzel, J., Raynaud, D., Barkov, N.I., Barnola, J.M., Basile, I., Bender, M., Chappellaz, J., Davis, J., Delaygue, G., Delmotte, M., Kotlyakov, V.M., Legrand, M., Lipenkov, V., Lorius, C., Pépin, L., Ritz, C., Saltzman, E., Stievenard, M., 1999, Climate and Atmospheric History of the Past 420,000 years from the Vostok Ice Core, Antarctica. Nature 399, 429-436.

Ronchail, J., Cochonneau, G., Molinier, M., Guyot, J.L., Goretti de Miranda Chaves, A., Guimarães, V., de Oliveira, E., 2002. Rainfall variability in the Amazon Basin and SSTs in the tropical Pacific and Atlantic oceans. Int. J. Climatol. 22, 1663-1686.

Sachse, D., Radke, J., Gleixner, G., 2004. Hydrogen isotope ratios of recent lacustrine *n*-alkanes record modern climate variability. Geochim. Cosmochim. Ac. 68, 4877-4889.

Sachse, D., Radke, J., Gleixner, G., 2006. δD values of individual *n*-alkanes from terrestrial plants along a climatic gradient - Implications for the sedimentary biomarker record. Org. Geochem. 37, 469-483.

Sauer, P., Eglinton, T.I., Hayes, J.M., Schimmelmann, A., Sessions, A., 2001. Compound-specific D/H ratios of lipid biomarkers from sediments as a proxy for environmental and climatic conditions. Geochim. Cosmochim. Ac. 65, 213-222.

Schefuß, E., Schouten, S., Schneider, R.R., 2005. Climatic controls on central African hydrology during the past 20,000 years. Nature 437, 1003-1006.

Sessions, A.L., Burgoyne, T.W., Schimmelmann, A., Hayes, J., 1999. Fractionation of hydrogen isotopes in lipid biosynthesis. Org. Geochem. 30, 1193-1200.

Sessions, A.L., 2006. Seasonal changes in D/H fractionation accompanying lipid biosynthesis in Spartina alterniflora. Geochim. Cosmochim Ac. 70, 2153-2162.

Sifeddine, A., Bertaux, J., Mourguiart, Ph., Disnar, J.R., Laggoun-Défarge, F., 1998. Etude de la sédimentation lacustre d'un site de forêt d'altitude des Andes centrales (Bolivie). Implications Paléoclimatiques. B. Soc. Geol. Fr. 169, 395-402.

Sifeddine, A., Martin, L., Turcq, B., Volkmer-Ribeiro, C., Soubiès, F., Campello Cordeiro, R., Suguio, K., 2001. Variations of the Amazonian rainforest environment: a sedimentological record covering 30,000 years. Palaeogeogr., Palaeoclim., Palaeoeco. 168, 221-235.

Sifeddine, A., Albuquerque, A.L.S., Ledru, M-P., Turcq, B., Knoppers, B., Martin, L., Zamboni de Mello, W., Passenau, H., Landim Dominguez, J.M., Campello Cordeiro, R., Abrao, J.J., Bittencourt, A.C., 2003. A 21000 cal years paleoclimatic record from Caçó Lake, northern Brazil: evidence from sedimentary and pollen analyses. Palaeogeogr., Palaeoclim., Palaeoeco. 189, 25-34.

Smith, F.A, Freeman, K.A., 2006. Influence of physiology and climate on δD of leaf wax n-alkanes from C3 and C4 grasses. Geochim. Cosmochim. Ac. 70, 1172–1187.

Stoecker, T.F., 2003. South dials north. Nature 424, 496-499.

Stuiver, M., Reimer, P.J., 1993. Extended 14C database and revised CALIB 3.0. ^{14}C age calibration program. Radiocarbon 35, 215-230.

Stuiver, M., Reimer, P.J., Braziunas, T.F., 1998. High-precision radiocarbon age calibration for terrestrial and marine samples. Radiocarbon 40, 1127-1151.

Turcq, B., Cordeiro, R.C., Sifeddine, A. Simoes Filho, F.F. Abrao, J.J., Oliveira, F.B.O., Silva, A.O., Capitaneo, J.L., Lima, F.A K, 2002. Carbon storage in Amazonia during the LGM: data and uncertainities. Chemosphere 49, 821-835.

van't Veer, R., Islebe, G.A., Hooghiemstra, H., 2000. Climatic change during the Younger Dryas chron in northern South America: a test of the evidence. Quat. Sci. Rev. 19, 1821-1835.

Wang, X., Auler, A.S., Edwards, R.L., Cheng, H., Cristalli, P., Smart, P.L., Richards, D.A., Shen, C.-C., 2004. Wet periods in northeastern Brazil over the past 210 kyr linked to distant climate anomalies. Nature 432, 740-743.

Yapp, C.J., Epstein, S., 1982. Climatic significance of the hydrogen isotope ratios in tree cellulose. Nature 297, 636-639.

Figure legends

Figure 1: Location of Lake Caçó site within the context of present day potential vegetation types encountered in northern Brazil. Open circles indicate the sites discussed in the text. The Lake Caçó lies in a shrub savanna (cerrado) corridor inserted between the dry savanna (caatinga) to the east and the humid rainforest to the west. The Present day positions of the InterTropical Convergence Zone (ITCZ) during the austral summer (DJF) and austral winter (JAS) are depicted with a dotted black line. The trajectory of moisture advection during austral summer is illustrated with a white arrow.

Figure 2: Age model for core MA-98-3 and sedimentation rates. The error bars represent the range of calibrated ages.

Figure 3: Variations of $\delta^{13}C$ (a) and δD values (b) for palmitic (δD_{PA}), behenic (δD_{BA}) and triacontanic (δD_{TA}) acids along the 20 ka sedimentary record of Lake Caçó. The error bars correspond to the standard deviation for duplicate ($\delta^{13}C$) and triplicate (δD) analyses. (c) Reconstructed hydrogen isotopic composition of the lake waters from δD_{PA} (δD_{watPA}) and δD_{BA} (δD_{watBA}) as calculated in paragraph 5.2. Lower values are interpreted as higher precipitation and reverse. (d) Evolution of the fractionation factor between lake waters (δD_{watPA}, calculated from δD_{PA}) and triacontanic acid ($\alpha_{TA/wat}$). Higher values indicate stronger evapotranspiration. VSMOW is Vienna Standard Mean Ocean Water. VPDB is Vienna Pee Dee Belemnite. PA is palmitic ($n-C_{16}$) acid; BA is behenic ($n-C_{22}$) acid and TA is triacontanic ($n-C_{30}$) acid.

Figure 4: Sketch diagram illustrating the sources of uncertainty when attempting to relate an isotopic signal measured on organic molecules retrieved form sedimentary archives with paleoclimatic parameters.

Figure 5: Comparison of the variations of paleohumidity in Lake Caçó with other proxy records for the last 20 ka. **a**, The δD_{TA} is the δD value for triacontanic acid, synthesised by terrestrial higher plants. It is interpreted as a proxy of relative humidity. Higher values correspond to drier conditions and reverse. **b**, The δD_{watPA} (δD of meteoric waters) is calculated from the δD of the palmitic acid (δD_{PA}) using a constant fractionation factor of 0.829 (see text and Huang et al., 2002). Low figures of δD_{watPA} correspond to

abundant precipitation. **c**, $\alpha_{TA/wat}$ is the coefficient of isotopic fractionation of hydrogen between leaf wax lipids and meteoric waters. High values of $\alpha_{TA/wat}$ correspond to intense evapotranspiration and reverse. **d**, Percentages of Myrtaceae pollen measured on another core from the same lake (MA-97-1). High percentages of Myrtaceae pollen indicate the development of a humid and warm forest. **e**, The AP/NAP ratio reflects the relative abundance of arboreal pollens (AP) and non-arboreal pollen (NAP) in the sample (Ledru et al., 2001; Sifeddine et al., 2003). Low AP values reflect the development of a savana whereas high values attest to the presence of a humid forest. **f**, Variations of the normalized Fe/Ca ratios obtained on several marine cores from north-eastern Brazil (Arz et al. 1998; Arz et al., 1999). Increased Fe/Ca ratios are interpreted as enhanced moisture supply over the north east of Brazil. **g**, Speleothems (white bars) and travertines (blackbars) growth phases in north-eastern Brazil, reflecting humid periods (Wang et al., 2004). **h**, Variations of the Amazon River outflow calculated from the oxygen isotopic composition ($\delta^{18}O$) of planktonic foraminifera in the sediments of the Amazon fan (Maslin and Burns, 2000). **i**, $\delta^{18}O$ in GRIP ice core (North Greenland Ice Core Project members, 2004). **j**, Deuterium in Vostok ice core (Petit et al., 1999). The location of the sites from which **f**-**h** records were obtained is indicated in Figure 1. YD is Younger Dryas and LGM is Last Glacial Maximum.

Table captions

Table 1: Radiocarbon ages of total organic matter from core MA-98-3.

Code	Sample depth	Measured ages ^{14}C yrs BP	$\delta^{13}C$	Conventional ages ^{14}C BP	Calibrated ages yrs BP	Intercept yrs BP
Beta – 162661	73-75	4930±50	-27.2 ‰	890±50	5720 to 5580	5610
Beta – 162662	196-198	9850±70	-28.9 ‰	9790±70	11270 to 11120	11200
Beta – 162663	286-288	14450±80	-27.8 ‰	14400±80	17680 to 16830	17250
Beta – 162664	354-356	15620±80	-19.9 ‰	15700±80	19230 to 18290	18750
Beta – 162665	426-428	16100±80	-22.9 ‰	16130±80	19740 to 18770	19240
Beta – 162666	574-576	16670±100	24.3 ‰	16670±100	20410 to 19330	19860

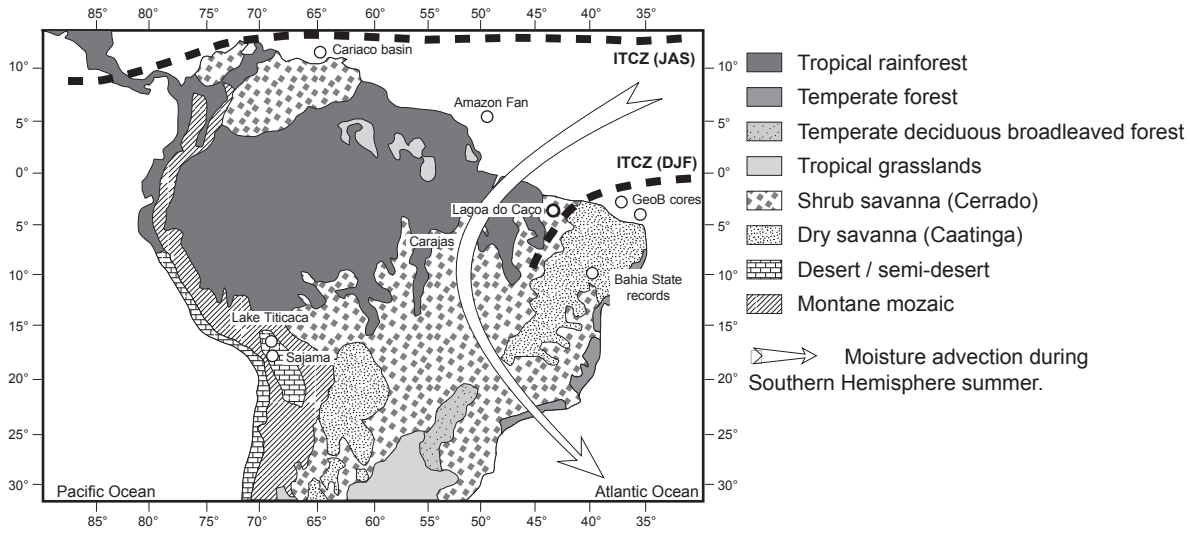
85° 80° 75° 70° 65° 60° 55° 50° 45° 40° 35°
10° 5° 0° 5° 10° 15° 20° 25° 30°
Cariaco basin
ITCZ (JAS)
Amazon Fan
ITCZ (DJF)
GeoB cores
Lagoa do Caco
Carajas
Bahia State records
Lake Titicaca
Sajama
Pacific Ocean
Atlantic Ocean
Tropical rainforest
Temperate forest
Temperate deciduous broadleaved forest
Tropical grasslands
Shrub savanna (Cerrado)
Dry savanna (Caatinga)
Desert / semi-desert
Montane mozaic
Moisture advection during Southern Hemisphere summer.

Figure 1

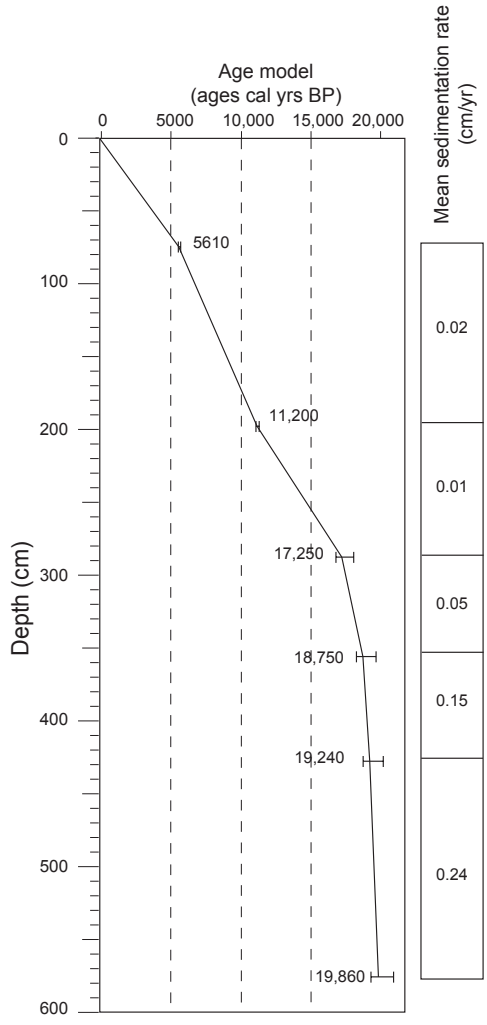
Age model
(ages cal yrs BP)
0
5000
10,000
15,000
20,000
Depth (cm)
0
100
200
300
400
500
600
5610
11,200
17,250
18,750
19,240
19,860
Mean sedimentation rate
(cm/yr)
0.02
0.01
0.05
0.15
0.24

Figure 2

Figure 3

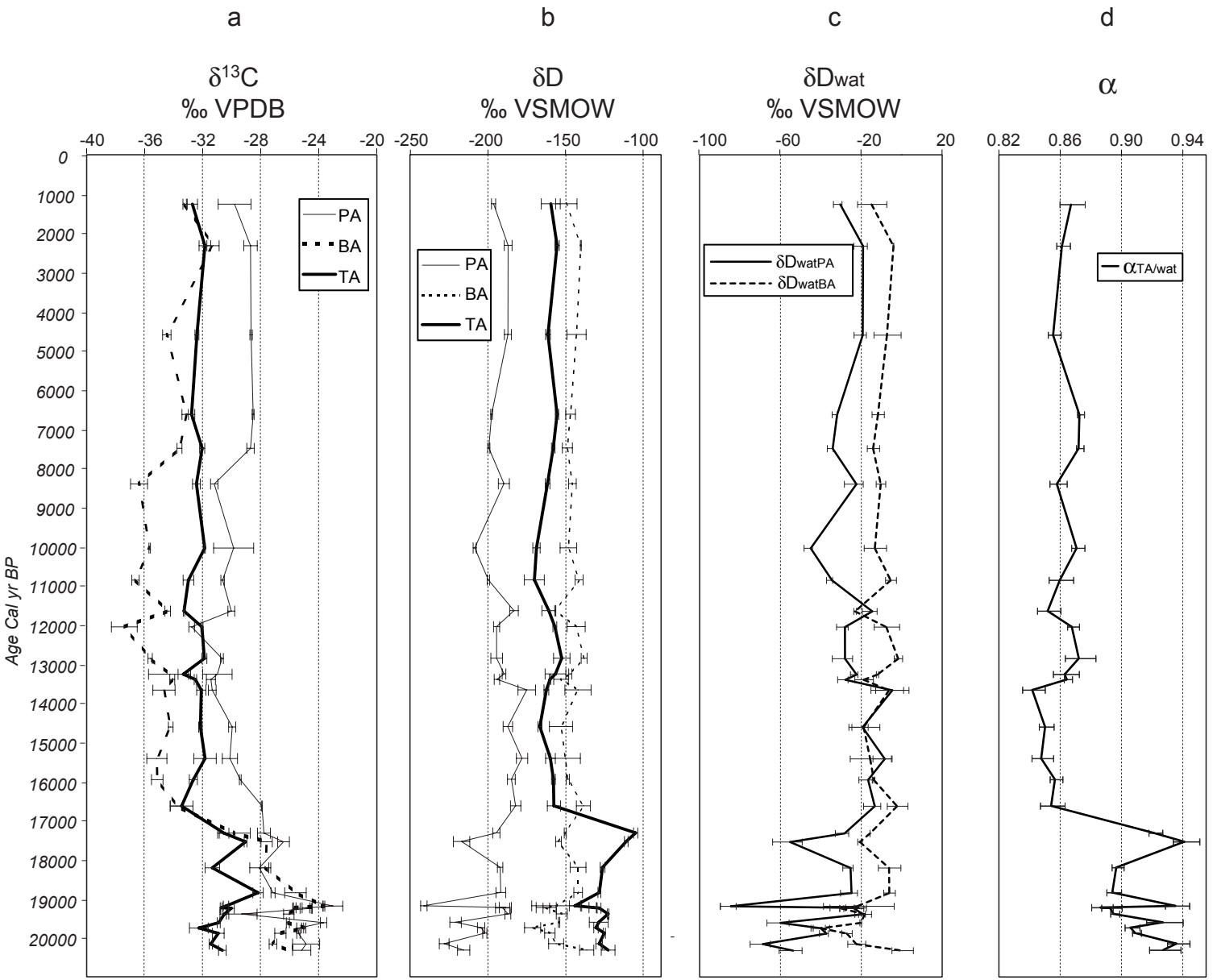
a
b
c
d
δ13C
‰ VPDB
δD
‰ VSMOW
δDwat
‰ VSMOW
α
-40 -36 -32 -28 -24 -20
-250 -200 -150 -100
-100 -60 -20 20
0.82 0.86 0.90 0.94
0 1000 2000 3000 4000 5000 6000 7000 8000 9000 10000 11000 12000 13000 14000 15000 16000 17000 18000 19000 20000
Age Cal yr BP
PA
BA
TA
PA
BA
TA
δDwatPA
δDwatBA
αTA/wat

Figure 4

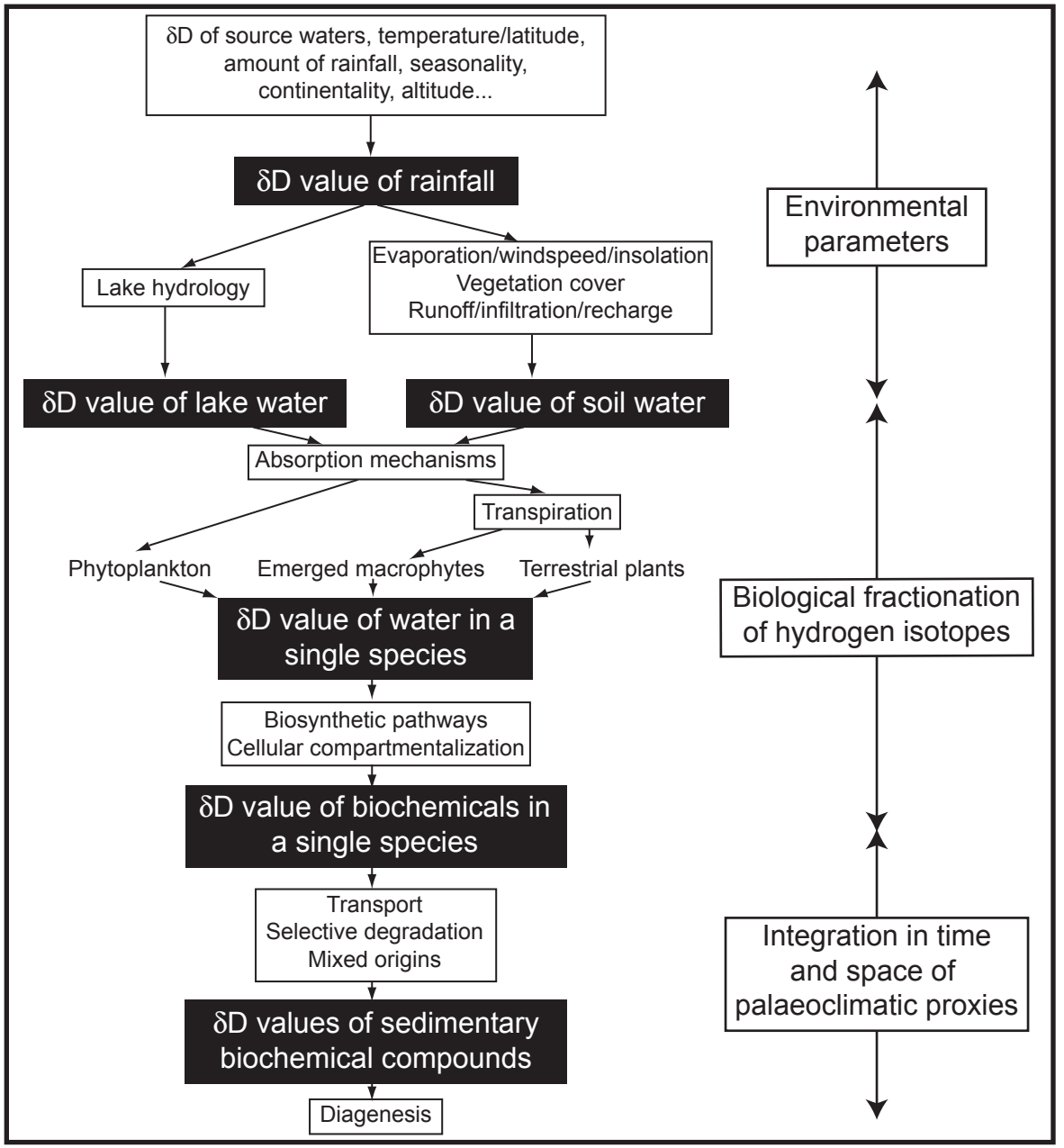
δD of source waters, temperature/latitude, amount of rainfall, seasonality, continentality, altitude...
δD value of rainfall
Lake hydrology
Evaporation/windspeed/insolation
Vegetation cover
Runoff/infiltration/recharge
δD value of lake water
δD value of soil water
Absorption mechanisms
Transpiration
Phytoplankton
Emerged macrophytes
Terrestrial plants
δD value of water in a single species
Biosynthetic pathways
Cellular compartmentalization
δD value of biochemicals in a single species
Transport
Selective degradation
Mixed origins
δD values of sedimentary biochemical compounds
Diagenesis
Environmental parameters
Biological fractionation of hydrogen isotopes
Integration in time and space of palaeoclimatic proxies

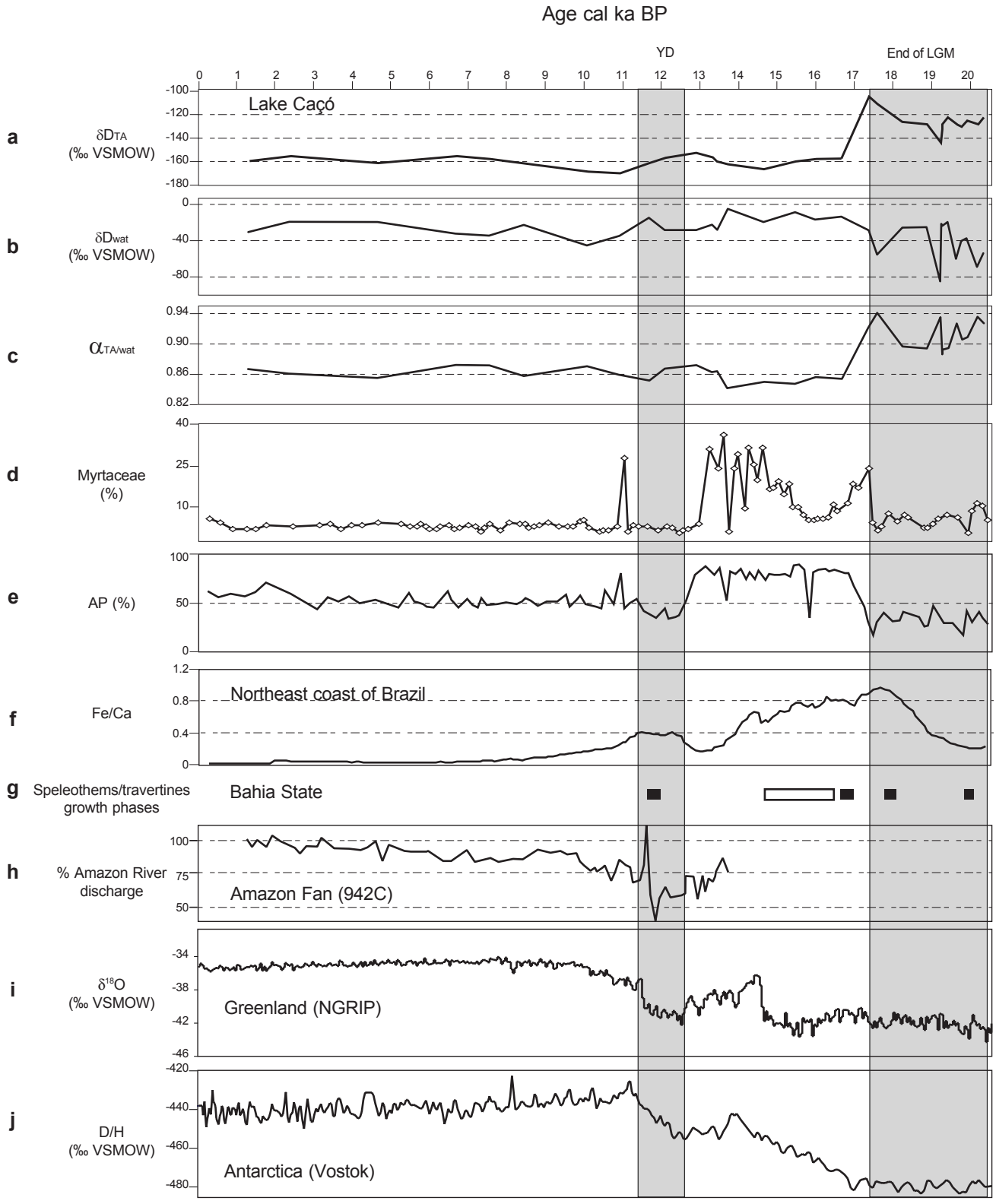
Age cal ka BP
YD
End of LGM
0 1 2 3 4 5 6 7 8 9 10 11 12 13 14 15 16 17 18 19 20
a
δDTA (‰ VSMOW)
-100 -120 -140 -160 -180
Lake Caçó
b
δDwat (‰ VSMOW)
0 -40 -80
c
αTA/wat
0.94 0.90 0.86 0.82
d
Myrtaceae (%)
40 25 10
e
AP (%)
100 50 0
f
Fe/Ca
1.2 0.8 0.4 0
Northeast coast of Brazil
g
Speleothems/travertines growth phases
Bahia State
h
% Amazon River discharge
100 75 50
Amazon Fan (942C)
i
δ18O (‰ VSMOW)
-34 -38 -42 -46
Greenland (NGRIP)
j
D/H (‰ VSMOW)
-420 -440 -460 -480
Antarctica (Vostok)

Figure 5